POLİTEKNİK DERGİSİ

JOURNAL of POLYTECHNIC

ISSN: 1302-0900 (PRINT), ISSN: 2147-9429 (ONLINE)
URL: http://dergipark.org.tr/politeknik

Comparison of the effects of magnetite nanoparticles on performance in a finned and finless liquid-air heat exchanger

Manyetit nanopartiküllerin kanatçıklı ve kanatçıksız sıvı-hava ısı eşanjöründe performansa etkisinin karşılaştırılması

Yazar(lar) (Author(s)): *Fauzi SHTEWİ[1], Mehmet ÖZKAYMAK[2], Khaled HAGİG[3], Abdelkerim FAHED[4], Faruk KILIÇ[5], Mustafa GÖKTAŞ[6], Nurettin ELTUĞRAL[7], Mustafa AKTAŞ[8]*

ORCID[1]: 0000-0002-4846-1776 *ORCID[4]: 0000-0003-1995-7630* *ORCID[7]: 0000-0001-6393-9611*

ORCID[2]: 0000-0002-4575-8988 *ORCID[5]: 0000-0002-9978-1972* *ORCID[8]: 0000-0003-1187-5120*

ORCID[3]: 0000-0001-5359-5608 *ORCID[6]: 0000-0001-8742-9114*

To cite to this article: *Shtewi F., Özkaymak M., Hagig K., Fahed A., Kılıç F., Göktaş M., Eltuğral N., and Aktaş M., "Comparison of The Effects of Magnetite Nanoparticles on Performance in A Finned and Finless Liquid-Air Heat Exchanger",* ***Journal of Polytechnic***; 29(4):290447:1-12 (2026).

Bu makaleye şu şekilde atıfta bulunabilirsiniz: *Shtewi F., Özkaymak M., Hagig K., Fahed A., Kılıç F., Göktaş M., Eltuğral N. ve Aktaş M., "Comparison of The Effects of Magnetite Nanoparticles on Performance in A Finned and Finless Liquid-Air Heat Exchanger",* ***Politeknik Dergisi***, 29(4):290447:1-12 (2026).

Erişim linki (To link to this article): http://dergipark.org.tr/politeknik/archive

DOI: 10.2339/politeknik.1605687

Comparison of The Effects of Magnetite Nanoparticles on Performance in A Finned And Finless Liquid-Air Heat Exchanger

Highlights

- *Thermal performance was analyzed in a double-pipe heat exchanger (DPHE) using magnetite nanoparticles in liquid-air heat exchanger.*
- *Examining the effect of using fins to the outer surface of the inner tube in heat exchanger on heat transfer.*
- *Comparing the effect of using magnetite nanoparticles and fins on heat transfer when the working fluid is air and water.*

Graphical Abstract

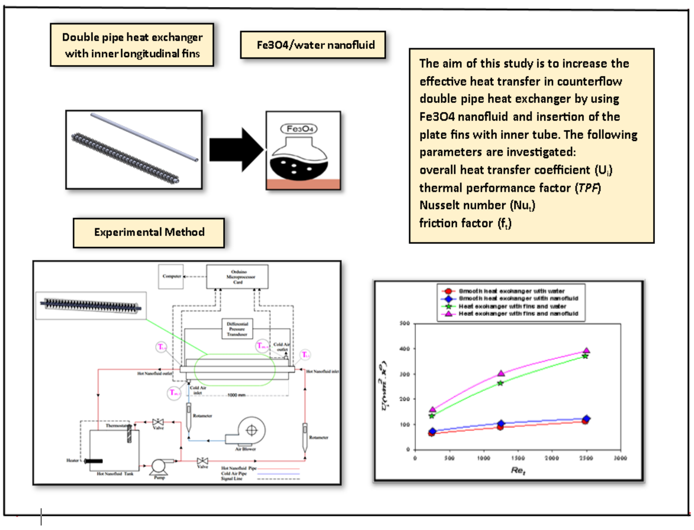

Figure. Schematic diagram of the experimental system**.**

Aim

The aim of the research is to examine the effect of using Fe_3O_4/water nanofluid on a finned and finless liquid-air heat exchanger, and to compare the results.

Design & Methodology

In the present work, the enhancement of heat transfer characteristics of Fe_3O_4/water nanofluid in a double pipe heat exchanger counter flow under laminar conditions ($249 < Re < 3000$) have been studied.Four experiments were conducted to compare the heat transfer performance enhancement of two different types of heat exchangers: one with nanofluid and plate fins (PF) inserts, and another with water alone.

Originality

Using nanofluid and fins in tandem to improve the concentric double-tube heat exchanger's performance is the main objective of this effort. For this reason, and in addition to using nanofluid as a primary fluid flow in the inner tube, our proposal is a heat exchanger design based on a concentric double tube by the insertion of aluminum plate fins.

Findings

A significant increase in heat transfer characteristics was observed, according to the results, given a constant volumetric concentration of nanofluid at varying Reynolds numbers, the finned tube heat exchanger has a 90–95% higher thermal performance factor than the plain tube heat exchanger.

Conclusion

The higher heat transfer rate of the finned tube heat exchanger is caused by the shape of the fins and the presence of nanofluids, also have a greater overall heat transfer coefficient compared to those containing water or a smooth tube.

Declaration of Ethical Standards

The authors of this article declare that the materials and methods used in this study do not require ethical committee permission and/or legal-special permission.

Comparison of The Effects of Magnetite Nanoparticles on Performance in A Finned And Finless Liquid-Air Heat Exchanger

Araştırma Makalesi / Research Article

Fauzi SHTEWI[1*] , Mehmet ÖZKAYMAK[2] , Khaled HAGIG[1] , Abdelkerim FAHED[3], Faruk KILIÇ[4], Mustafa GÖKTAŞ[5] , Nurettin ELTUĞRAL[6], Mustafa AKTAŞ[7]

[1]Department of Energy Systems Engineering , Karabük University , Karabük, Türkiye.
[2]Department of Mechatronics, Vocational School of Trade and Industry, Karatay University, Konya,Türkiye.
[3]Department of Mechanical Engıneering, Janzour College of Engineering Technology, Tripoli, Libya.
[4]Department of Mechanical Engineering, National Defence University, Ankara, Türkiye.
[5]Technical Sciences Vocational School, Gazi University, Ankara, Türkiye.
[6]Department of Biomedical Engineering , Karabük University , Karabük, Türkiye.
[7]Department of Energy Systems Engineering, Gazi University, Ankara, Türkiye.

(Geliş/Received :23.12.2024 ; Kabul/Accepted : 27.01.2025 ; Erken Görünüm/Early View : 11.02.2025)

ABSTRACT

Efforts are being made to improve heat transfer efficiency in many different contexts, with the help of nanofluids and expanded surfaces, among other things. Among them, a clever method to enhance heat transmission is to equip heat exchanger tubes with inner fins. The experimental study details the use of a nanofluid of iron oxide and water in a two-tube counterflow heat exchanger that has many longitudinal fins on the inside to induce convective heat transfer. The pressure drop and convective heat transfer enhancement are studied for a nanofluid moving in a horizontal circular tube with internal longitudinal fins under laminar conditions ($249 < Re < 3000$). Fe_3O_4 nanoparticles have a volumetric concentration that falls between $0 < \varphi < 0.5\%$. For different Reynolds numbers and a constant volumetric concentration of nanofluid, the results demonstrate that the finned tube heat exchanger outperforms the plain tube heat exchanger thermally by a factor of 90 to 95%. The Nusselt number ratio of the Fe_3O_4 water nanofluid increases with increasing Reynolds number. As the Reynolds number increases, the friction factor decreases and the pressure drop is larger in finned tube heat exchangers compared to plain tube heat exchangers due to the flow resistance provided by the fin form.

Keywords: Finned tube, Fe_3O_4 nanoparticles, nanofluid, heat transfer enhancement, thermal performance factor.

Manyetit Nanopartiküllerin Kanatçıklı ve Kanatçıksız Sıvı-Hava Isı Eşanjöründe Performansa Etkisinin Karşılaştırılması

ÖZ

Çeşitli ortamlarda ısı transfer verimliliğini artırmak için nanofluidler ve genişletilmiş yüzeyler kullanmak da dahil olmak üzere çok sayıda girişim devam etmektedir. Bunlar arasında, ısı değiştirici tüplerine iç kanatçıklar eklemek ısı transferini iyileştirmenin akıllıca bir yoludur. Bu çalışma, birkaç iç uzunlamasına kanatçığa sahip çift borulu karşı akışlı bir ısı değiştiricide Fe_3O_4 -su nanofluidini kullanarak zorlanmış konvektif ısı transferinin deneysel bir araştırmasını açıklamaktadır. Laminer koşullar altında ($249 < Re < 3000$) iç uzunlamasına kanatçıklara sahip yatay dairesel bir tüpte akan nanofluid için, basınç düşüşü ve konvektif ısı transferi iyileştirmesi incelenmiştir. Fe_3O_4 nanopartiküllerinin hacimsel konsantrasyonu $0 < \varphi < 0{,}5\%$ aralığındadır. Bulgular, kanatçıklı borulu ısı değiştiricinin, sabit hacimsel nanofluid konsantrasyonuna sahip değişen Reynolds sayıları için basit borulu ısı değiştiriciden %90-95 daha yüksek bir termal performans faktörüne sahip olduğunu göstermektedir. Fe_3O_4 -su nanofluidinin Nusselt sayı oranı Reynolds sayısı arttıkça artar. Çünkü kanatçık şekli akış direnci sağlar, Reynolds sayısı arttıkça sürtünme faktörü azalır ve basınç düşüşü kanatçıklı borulu ısı değiştiricilerde düz borulu ısı değiştiricilere göre daha fazladır..

Anahtar Kelimeler: Kanatçıklı borulu, Fe_3O_4 nanopartiküllerinin, ısı transferi iyileştirmesi, termal performans faktörü.

1. INTRODUCTION

Recovering heat from waste and refining hydrocarbons both rely heavily on heat exchangers. Heat exchangers designed to increase heat transmission using cutting-edge technologies are having an ever-increasing effect on the process sectors. Tubes can have fins attached to either the inside or outside of the tube, or both sides. Power stations, oil and gas refineries, and waste heat recovery systems all make use of finned tube heat exchangers. Internal fins in tubes enhance the effective heat transfer area and, by extension, the heat transfer rate, as discussed by Watkinson et al. [1,2]. Maxwell [3] investigated this method in depth, and it has recently been approved as a means to improve heat transmission by dispersing

**Sorumlu Yazar (Corresponding Author)*
e-posta : fauzishtewi1968@gmail.com

metallic particles into the base fluid. Tests on concentric tube heat exchangers for water with different concentrations of nanoparticles in the base fluids were conducted by Shriram S. Sonawane, Kailas L. Wasewar, et al. [4].They found that 3% nanofluids performed optimally, with an overall heat transfer coefficient that was 16% higher than water. Baba, Muhammad Sikindar et al. [5]. This work describes an experimental investigation of forced convective heat transfer utilising a Fe_3O_4/water nanofluid in a double tube counterflow heat exchanger with several interior longitudinal fins. The findings show that for the higher volumetric heat exchanger, the finned tube heat exchanger has an 80–90% higher heat transfer rate than the plain tube heat exchanger.

In comparison to the water data, Zamzamian et al.[6] found that heat transfer was enhanced by 26%, 38% for 1.0 weight percent of Al_2O_3 nanofluid and 37%, 49% for 1.0 weight percent of CuO nanofluid flow in a double pipe heat exchanger and plate heat exchanger, respectively.

A stable laminar heat transfer in circular tubes with internal fins and a continuous heat flow was the topic of Iftakhar and Ghoshdastidar's numerical simulation [7]. The findings demonstrate that the interior fins significantly increased heat transmission. Multi-scale annular fins attached to a pin fin were designed optimally by Mohammad Reza Hajmohammadi [8]. The assembly's geometric configuration is optimized using the Genetic Algorithm and the direct search approach. The optimization findings show that the assembly's thermal performance is significantly improved by increasing the number of geometrical variables. Webb, Scott, et al. [9] offered a parametric study of the efficiency of turbulent forced convection in heat exchangers using internal ultrafine tubes.

Experimentally compact slit fin exchangers with plain and louvred fins were examined by Wang et al. [10]. In line with earlier research, it was discovered that while louvred fins increased heat transfer, the number of rows had only a slight impact on frictional performance

By altering the flow direction, Dr. Khalid Faisal Sultan [11] showed how oxide zirconium-oil nanofluids and silver can improve heat transfer in a heat exchanger with or without fins. To improve heat transfer, the nanofluid was used in a heat exchanger with and without fins. According to the measured results, using oil nanofluid with silver enhances heat transfer the most when compared to using oxide zirconium nanofluid.

Sheu and Tsai [12] used three-dimensional numerical analysis to examine the efficiency of enlarged fins in a finned tube heat exchanger with two rows of fins. The optimal design, according to Hajmohammadi [13], consists of tree-shaped inverted fins that are punctured into heat-generating objects in order to accelerate the heat transfer rate. The optimization findings show that the optimized tree-shaped design works better than the single-root cavities given in the open literature. The heat transfer characteristics of a fully developed laminar forced convection flow in an internal triangle-shaped fined circular tube were studied by Masliyah and Nandakumar [14]. The axially uniform heat flow and peripherally uniform temperature were generated using the finite element approach. Hajmohammadi et al. [15] assumed the boundary condition of slide and proved the optimal geometric design of a micro-scale channel heat sink. The three-dimensional fluid flow and heat transport processes inside the microchannel heat sink are investigated using numerical analysis. Under turbulent flow conditions, Duangthongsuk and Wong Wises [16] investigated how a TiO_2 water nanofluid improved heat transfer in a horizontal double tube counterflow heat exchanger. Wen and Ding [17] demonstrated that an increase in Reynolds number and volume concentration led to an improvement in heat transfer using an Al_2O_3 water nanofluid flowing through a copper tube. Sundar and Naik et al. [18] found that the heat transfer coefficient improved when they used a circular tube filled with a Fe_3O_4 magnetic nanofluid. The use of Fe_3O_4 kerosene nanofluid increased heat transfer in a simple tube, according to Yu & Xie et al. [19].

Prior research suggests that the synergistic effects of nanofluids and surface modification methods have received less consideration. Furthermore, no research has been conducted on the heat transfer and friction qualities when an annulus with plat fins and an inner pipe running with a 0.5% volume concentration of Fe_3O_4 nanofluid are coupled. Consequently, this work seeks to fill this information vacuum by experimentally studying the thermal performance of a concentric double-tube heat exchanger that uses nanofluid and fins at the same time. In addition to the 0.5% volume concentration of Fe_3O_4 nanofluid flowing in the inner pipe, the effect of plate fins dispersed around the outer circumference of the inner pipe in the cold air stream on heat transfer will be studied.

To evaluate the effectiveness of the proposed setup, we will mainly look at four thermal characteristics: the total heat-transfer coefficient, the Nusselt number, the friction factor, and the thermal performance factor. After that, for every setup, we'll check the relationships between the Reynolds and friction factors, Nusselt and Reynolds numbers, and the total heat transfer coefficient. One last thing to consider while assessing the situation is the thermal performance improvement factor (TPF).

2. MATERIAL and METHOD

2.1. Nanofluid Preparation and Properties

Fe_3O_4 nano particles of 200 nm diameter are combined in a predetermined amount with the base fluid (water) to achieve the necessary volumetric concentration of nanofluid. Sonicating the nanofluid with an ultrasonic vibrator ensures complete particle dispersion. The density, viscosity, specific heat, and thermal conductivity of the nanofluid are displayed in table 1.

Table 1. Magnetite nanoparticles' physical characteristics [20]

Submicron particle	Mean diameter	Density (kg/m^3)	Specific Surface(m^2/g)	Thermal condutivity (w/m.k)	Specific heat(j/kg.k)
Fe_3O_4	200nm	5180	60	9.7	670

2.2. Numerical Procedure

An illustration of the experimental setup may be seen in Figure 1. It has a testing space, two systems for hot nanofluids and cold air flows with their attachments, and so on. In addition to the devices used to measure pressure, temperature, and flow. A 1000 mm long counterflow double pipe heat exchanger serves as the test portion. An external diameter of 110 mm and an interior diameter of 106 mm characterize the PVC outer tube (annulus). It has a layer of glass fiber wool applied to it. The inner tube is 26 mm in diameter with an outside diameter of 30 mm and is made of aluminum.

First, hot Fe_3O_4 nanofluid with a volume concentration of 0.5 percent flows through the inner tube; second, chilly air flows through the shell; and they constitute the working fluids in this system. The hot nanofluid circuit consists of the following components: a heat exchanger's inner tube, a centrifugal pump with 0.41, 0.30, and 0.18 horsepower, a Rotameter, a variable area flow meter (0.2-2 lpm) that has been calibrated by calculating the time needed to fill a 10-L capacity vessel, and a hot nanofluid reservoir coupled with an electrical heater and thermostat that has an accuracy of ± 0.2 C°.

An 81-W air blower, a calibrated variable area air flow meter (Rotameter) with a range of 200–2000 lpm and a measuring accuracy of ± 2%, and the heat exchanger's outer tube (annulus) make up the cold air circuit. The data logger, which is an Arduino microcontroller card, is equipped with K-type thermocouples that measure the input and output temperatures of the hot nanofluid and cold air, respectively. A mercury-in-glass thermometer with a precision of ±0.2 C° was used to calibrate each thermocouple in the laboratory. The pressure drop of the hot nanofluid stream between the input and output of the inner tube is monitored using a differential pressure transducer that has a working range of 0-100 Psi and an accuracy of ± 2% of full scale.

2.3. Technical Details of The Plate Fins (PF)

Using nanofluid and fins in tandem to improve the concentric double-tube heat exchanger's performance is the main objective of this effort. For this reason, and in addition to using nanofluid as a primary fluid flow in the inner tube, our proposal is a heat exchanger design based on a concentric double tube by the insertion of aluminum plate fins (PF), which are the same material of inner tube of heat exchanger, into the outer tube (annulus) in the stream of cold air. They were distributed as 30 rings along the entire outer perimeter of the inner tube so that they form 90 angles with it. Fig. 2a shows the geometrical configuration and the dimensions of plate fins (PF) inserted. Each of the 30 rings contains 14 plate fins with dimensions height HPF = 30 mm, width WPF = 5 mm and thickness tPF = 1 mm where they have been drawn on aluminum annulus with an inner circle diameter of 28 mm and an outer circle diameter of 90 mm evenly distributed on this annulus using SolidWorks software, and then milled using a CNC machine. Using a press-fit bounding approach, the current study presses aluminum fin rings into annular grooves (gaps) that wrap around the full circumference of the tube and open on the outside wall of the inner aluminum tube of the heat exchanger. The grooves have a depth of 1 mm and a width of 1 mm. Thirty annular grooves (gaps) are drawn by SolidWorks software and milled by a milling CNC machine, to ensure that the aluminum plate fins (PF) are placed at the desired position around the outer wall of inner aluminum tube to reduce the contact resistance. The insertion of the plate fins (PF) with inner tube into the outer tube (annulus) is considered as a loose-fit, where the plate fins (PF) with inner tube has the geometrical dimensions of diameter (dPF)= 90 mm with the clearance to the outer tube (annulus) wall (dan, i − dPF) / 2 = c = 8 mm as shown in the Fig. 2b.

2.4. Experimental Procedures

All instruments are calibrated before their installation in the experimental setup, then the nanofluid was heated in the tank that contained the electric heater and thermostat to maintain the constant temperature of nanofluid. Using two separate temperatures 40 and 50 °C, the nanofluid was heated in the tank before being allowed to enter the inner tube of the exchanger by a pump.

Experimental conditions included three distinct flow rates (0.2, 1, and 2 L/min) and a Reynolds range ($249 \le Re \le 3000$) controlled by the hot nanofluid's adjustable flow meter. A constant airflow rate of 1250 L/min was maintained throughout the experiments, with the temperature of the laboratory room being adjusted using the installed digital heating system.

The air blower was used to force cold air from the room into the outer pipe (annulus) with Tan,i = 22.5 °C.

This heat exchanger has a counter flow configuration. Once the system reached a steady state, I recorded the temperatures at various locations on the Arduino microcontroller board. Additionally, I measured the pressure drop of the hot nanofluid stream between the inner tube intake and outflow at a test section.

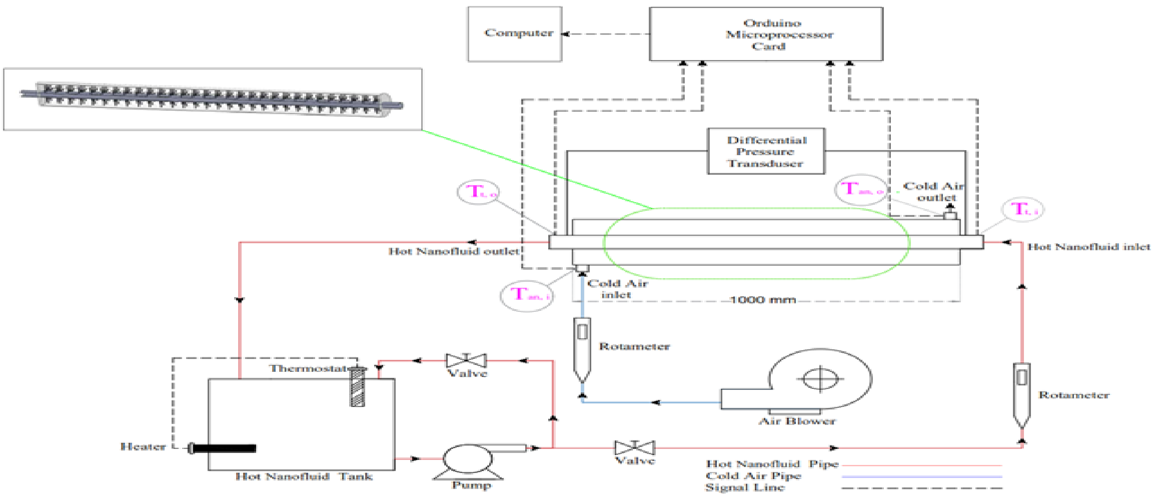

Figure 1. Experimental setup schematic diagram.

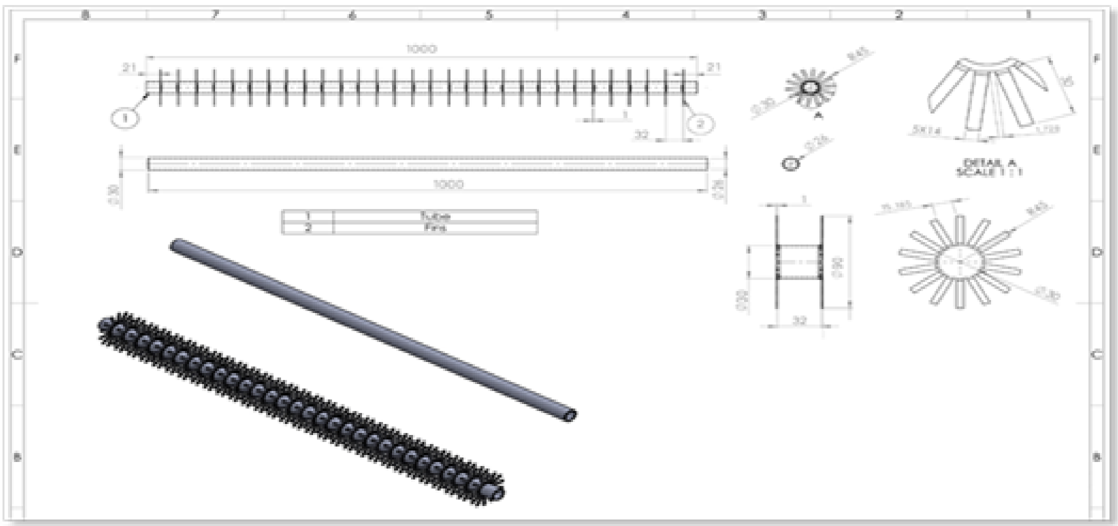

Figure 2a. Schematic sketch of the plate fins details (PF).

Table 2 shows the range of operating conditions for nanofluid, water, and air. Four experiments were conducted to compare the heat transfer performance enhancement of two different types of heat exchangers: one with nanofluid and plate fins (PF) inserts, and another with water alone. All the experiments used similar flow and operating conditions. In the first trial, the smooth heat exchanger was filled with water but did not have PF. Using a volume concentration of 0.5%, the second experiment's inner tube was filled with Fe_3O_4 nanofluid. In the third experiment, the cold air stream was passed through an outer tube that contained (PF) and water via an inner tube. The last experiment employed the same positioning of PF and the usage of Fe_3O_4 nanofluid in the inner tube as the third, with a volume concentration of 0.5%. In Figure 3, we can see the image of the plate fins (PF) that were placed in the annulus. We also computed a variety of thermal metrics, including the total heat-transfer coefficient, heat transfer (Nusselt number), friction factor (f), and thermal performance factor (TPF).

Afterwards, for all configurations, we checked for correlations between Reynolds and the total heat transfer coefficient, Nusselt numbers and Reynolds, and the friction factor. Lastly, the thermal performance enhancement factor (TPF) was used to evaluate the examples that were analyzed.

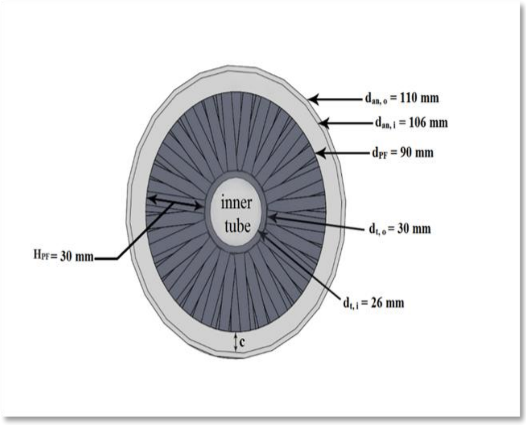

Figure 2b. Cross-sectional view of the plate fins (PF) inserts

Figure 3. The photograph of plate fins.

Table 2. Operating conditions for the range of both fluids

Operating conditions and parameters	Value or Range
Internal pipe-side	
Water flow rate, l/min	0.2,1, and 2 lpm (236 ≤ Ret < 3000)
Inlet temperature, °C	40,50 °C
Nanofluid flow rate, l/min	0.2,1, and 2 lpm (249 ≤ Ret < 3000)
Inlet temperature, °C	40,50 °C
Annulus-side	
Air flow rate, l/min	1250 lpm (Re_{an} ≈ 12684)
Inlet temperature, °C	22.5 °C

in annulus.

2.5 Calculations

As a first step, we calculated the thermophysical properties of the annulus's cold air and the inner tube's hot water at mean temperatures, $T_{t,m}$ and $T_{an,m}$, respectively.

$$T_{t,m} = (T_{t,i} + T_{t,0})/2 \tag{1}$$

$$T_{an,m} = (T_{an,i} + T_{an,0})/2 \tag{2}$$

For heat transfer calculations, the most important parameters to consider are the inlet and exit temperatures of the hot water and cold air streams, as well as their respective test section flow rates. The inner tube and annulus sides heat transfer rates (Q_t, Q_{an}) were calculated using the following formula:

On the inner tube side, the heat was transmitted from the hot water.

$$Q_t = \dot{m}_t\, Cp_t\left(T_{t,i} - T_{t,o}\right) \tag{3}$$

On the annulus side, the heat was transmitted to the cold air.

$$Q_{an} = \dot{m}_{an}\, Cp_{an}\left(T_{an,o} - T_{an,i}\right) \tag{4}$$

To calculate the internal convective heat transfer coefficient, the average heat transfer rates for the two sides—cold air on the annulus side and hot water on the inner tube side—were found:

$$Q_{ave} = \frac{|Q_t| + |Q_{an}|}{2} \tag{5}$$

Since we know the fluid's inlet and exit flow temperatures, we can calculate its heat transfer coefficient using the logarithmic mean temperature difference (LMTD). The following formula is used to calculate the mean logarithmic temperature (LMTD):

$$\Delta T_{LMTD} = \frac{\Delta T_i - \Delta T_o}{\ln\left[\frac{\Delta T_i}{\Delta T_o}\right]} = \frac{(T_{t,i} - T_{an,o}) - (T_{t,o} - T_{an,i})}{\ln\left[\frac{(T_{t,i} - T_{an,o})}{(T_{t,o} - T_{an,i})}\right]} \tag{6}$$

Equation (7) was used to determine the total heat transfer coefficient (Ui), which is dependent on the inner tube's surface area.

$$U_i = \frac{Q_{ave}}{A_{t,i}\,\Delta T_{LMTD}} \tag{7}$$

The inner tube's surface area is denoted as $A_{t,i}$.

$$A_{t,i} = \pi d_{t,i}\, L_t \tag{8}$$

By expressing the total heat transfer coefficient (U_i) in terms of the thermal resistances, the following may be done to estimate the tube side heat transfer coefficient (h_t) without disregarding the conduction thermal resistance of the aluminum tube wall:

$$\frac{1}{U_i A_{t,i}} = \frac{1}{h_t A_{t,i}} + \frac{\ln\left(d_{t,o}/d_{t,i}\right)}{2\pi k L} + \frac{1}{h_{an} A_{t,o}} \tag{9}$$

To get the average Nusselt number on the annulus side, the turbulent air flow was modeled using the well-known Dittus-Boelter [21] correlation for fully developed turbulent flow (Nu_{an}), Eq. (10):

$$Nu_{an} = 0.023\, Re_{an}^{0.8} Pr_{an}^{0.4} \tag{10}$$

Following that, the following is the average heat transfer coefficient for the annulus-side fluid, h_{an}:

$$h_{an} = \frac{Nu_{an}\, k_{air}}{d_{an,h}} \tag{11}$$

About which, $d_{an,\,h}$ = The hydraulic diameter of the annulus. It is worth noting that the simple annulus's hydraulic diameter is the same as:

$$d_{an,h,plainannulus} = d_{an,i} - d_{t,o} \tag{12}$$

Using the usual concept of the annulus hydraulic diameter (4Vflow / Awet), the diameter was computed with PF inputted (dan, h). As shown in Figure 3b, two flow streams on the annulus side were considered: the annular flow in the clearance above the PF tip (c) and the annular flow between the plate fins. As a result, the total flow volume will be:

$$V_{flow} = \left[\pi\left(d^2{}_{an,i} - d^2{}_{PF}\right) {}^{L_{an}}/_{4}\right] + \left[\pi\left(d^2{}_{PF} - d^2{}_{t,o}\right) {}^{L_{an}}/_{4}\right] - H_{PF}\, W_{PF}\, t_{PF}\, N_{PF} \tag{13}$$

For the annulus's inner wetted wall, the flow's wetted area is ($\pi\, d_{an,i}\, L_{an}$); for the inner tube's outer wetted wall, it's [$\pi\, d_{t,o}\, L_t + 2\,(H_{PF}\ W_{PF}\ N_{PF} + H_{PF}\ t_{PF}\ N_{PF})$], and for plate-fin surfaces, it's [$\pi\, d_{t,o}\, L_t$]. Hence, the hydraulic diameter of the flow stream was calculated using Eq. (14).

$$d_{an,h} = \frac{4V_{flow}}{A_{wet}} = \frac{[\pi(d^2{}_{an,i} - d^2{}_{PF})L_{an}] + [\pi(d^2{}_{PF} - d^2{}_{t,o})L_{an}] - 4\, H_{PF}\, W_{PF} t_{PF} N_{PF}}{\pi(d_{an,i}L_{an} + d_{t,o}L_t) + 2(H_{PF}\, W_{PF} N_{PF} + H_{PF}\, t_{PF} N_{PF})} \tag{14}$$

So, to determine Nu_t, the mean Nusselt number for the fluid on the tube's outside, the following formula was employed:

$$Nu_t = \frac{h_t d_{t,i}}{k_{water}} \tag{15}$$

The following formulas can be used to determine the Reynolds numbers of tubes and annuli, respectively:

$$Re_t = \frac{\rho_{water} u_t\, d_{t,i}}{\mu_{water}} \tag{16}$$

$$Re_{an} = \frac{\rho_{air}\, u_{an}\, d_{an,h}}{\mu_{air}} \tag{17}$$

where: u_t =($V_{water}/A_{c,\,t}$), $A_{c,\,t}$ is a Cross-sectional area for Inside tube ($A_{c,t} = \frac{\pi}{4} d^2{}_{t,i}$). u_{an} = (V_{air} /$A_{c,\,an}$), $A_{c,\,an}$ is a Cross-sectional area for annulus $\left[A_{c,an} = \frac{\pi}{4}\left(d^2{}_{an,i} - d^2{}_{t,o}\right)\right]$.

In this investigation, the fluid's Darcy friction factor was determined using the following equation (18) based on observations of the flow pressure decrease in the tube-side that occurred simultaneously with the heat transfer data:

$$f_t = \frac{\Delta P}{\left({}^{\rho u_t^2}/_{2}\right)\left({}^{L_t}/_{d_{t,i}}\right)} \tag{18}$$

Good heat performance is defined as the ability to substantially enhance the rate of heat transfer while keeping the increase in pressure drop to a minimum. The thermal performance improvement factor denotes this and is calculated as the ratio of the Nusselt number to the friction ratio. In order to evaluate the inserts' performance, the thermal performance augmentation factor has been calculated.

$$TPF = \frac{\left({}^{Nu_t}/_{Nu_{st}}\right)}{\left({}^{f_t}/_{f_{st}}\right)^{1/3}} \tag{19}$$

The accuracy and repeatability of measurements are critical to the validation of experimental work. The primary goal of calculating uncertainty is to arrive at a range of confidence levels. The dispersion of measurement results caused by variables and characteristics that either directly or indirectly affect the results is known as uncertainty. Measurement factors like accuracy and precision are crucial because they reduce the uncertainty of the outcome. Kline and McClintock [22] explain how to calculate the parameter uncertainty by adding up the effects of all the inputs and taking the root of the result. The highest uncertainties in the primary parameters for each experimental run are compiled in Table 3.

The uncertainties of each of the parameters under investigation are computed using Equation (20).

Table 3. Maximum degree of uncertainty in the primary parameters

Parameters	Uncertainty (%)
Side of the anulus Reynolds number	± 2.2
Side of the anulus The Nusselt number	± 3.7
Coefficient of Annulus-side Heat Transfer	± 2.7
Reynolds number on the tube side	± 2.8
Average heat transfer	± 2.5
Total heat transfer coefficient	± 3.5
Tube-side The Nusselt number	± 3.2
Heat transfer coefficient at the tube side	± 3.35
Friction factor on the tube side	± 2.9
Enhancement factor for thermal performance	± 3.8

$$W_R = \pm\left[\left(\frac{\partial R}{\partial x_1}w_1\right)^2 + \left(\frac{\partial R}{\partial x_2}w_2\right)^2 + \ldots + \left(\frac{\partial R}{\partial x_n}w_n\right)^2\right]^{1/2} \quad (20)$$

where w is the uncertainty of the independent variables (measured tolerances) and (x_1, x_2, ..., x_n) are measured independent variables.

2.6 Validation of Present Experimental Results for Distilled Water

Using the aforementioned experimental procedures and analysis techniques, the methodology for calculating heat transfer coefficients and friction factors is validated by measuring the flow in the smooth tube and comparing the results to empirical heat transfer and friction factor correlations. The experimental techniques for heat transfer calculations were validated by comparing the Nut findings for hot water moving through the inner tube with the Sieder and Tate correlation [23].

Eq. (21) for Nut calculations in the laminar flow region, and the Gnielinski correlation [24], Eq. (22) for Nut calculations in the transient and turbulent flow region.

$$Nu_t = 1.86\left(\frac{Re_t Pr_t d_{t,i}}{L_t}\right)^{1/3}\left(\frac{\mu_b}{\mu_s}\right)^{0.14} \quad (21)$$

$$Nu_t = \frac{\left(f_t/8\right)(Re_t - 1000)Pr_t}{1 + 12.7\sqrt{f_t/8}\left(Pr_t^{2/3} - 1\right)}\left[1 + \left(d_{t,i}/L_t\right)^{2/3}\right] \quad (22)$$

For the smooth inner tube experiments performed at 40 °C and 50 °C, Figure 4 shows the changes in the Reynolds number and the Nusselt number, respectively. The experimental data collected at 40 and 50 degrees Celsius agree with empirical correlations results for the smooth tube, with an average deviation of less than ± 6.025% and ± 11.641% respectively for the Nusselt number.

Comparing the experimental methodologies with the results of allowed for validation of the tube-side friction factor ft estimates. Eq. (23) for the laminar flow region, and Filonenko correlation [26], Eq. (24) for the transient and turbulent flow region.

$$f_t = \frac{64}{Re_t} \quad (23)$$

$$f_t = (1.82\,logRe_t - 1.64)^{-2} \quad (24)$$

Figure 5 displays the relationship between the friction factors and Reynolds numbers for the smooth tube in two different temperature experiments: (a) at 40 °C and (b) at 50 °C. The

empirical correlations for the smooth tube agree with the experimental data collected at 40 and 50 degrees Celsius, with an average deviation of less than ± 6.6% and ± 8.32% respectively for the friction factor.

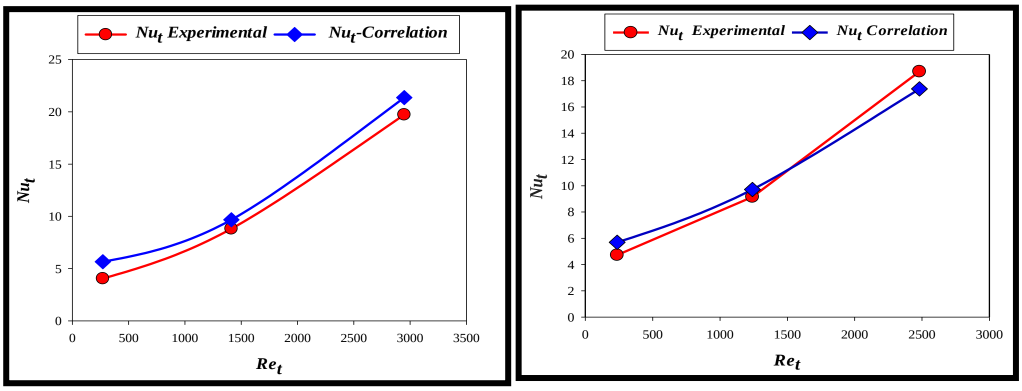

Figure 4. Comparison between the Nusselt number values versus the tubular Reynolds number of experimental and correlations results for the smooth tube: (a) experiments at $T_{t,i}$ = 40 °C, (b) experiments at $T_{t,i}$ = 50 °C

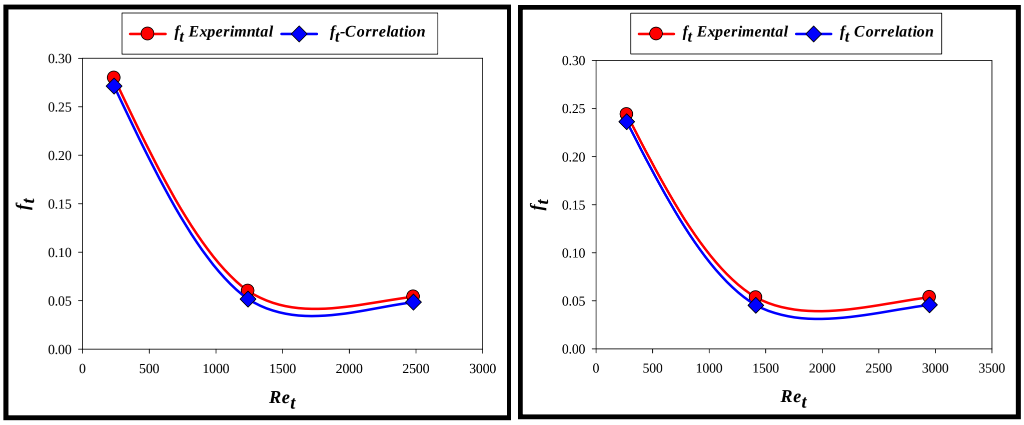

Figure 5. Comparison between the friction coefficient values versus the tubular Reynolds number of experimental and correlations results for the smooth tube: (a) experiments at $T_{t,i}$ = 40 °C, (b) experiments at $T_{t,i}$ = 50 °C.

2.7 Validation of Present Experimental Results for Nanofluids

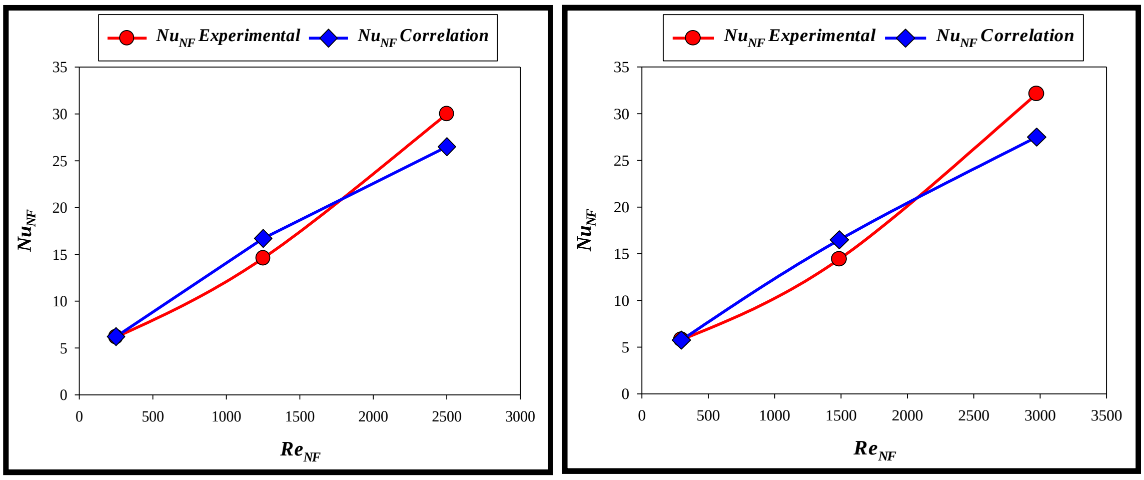

Figure 6. Comparison between the Nusselt number values versus the tubular Reynolds number of experimental and correlations results for the smooth tube: (a) experiments at $T_{t,i}$ = 40 °C, (b) experiments at $T_{t,i}$ = 50 °C.

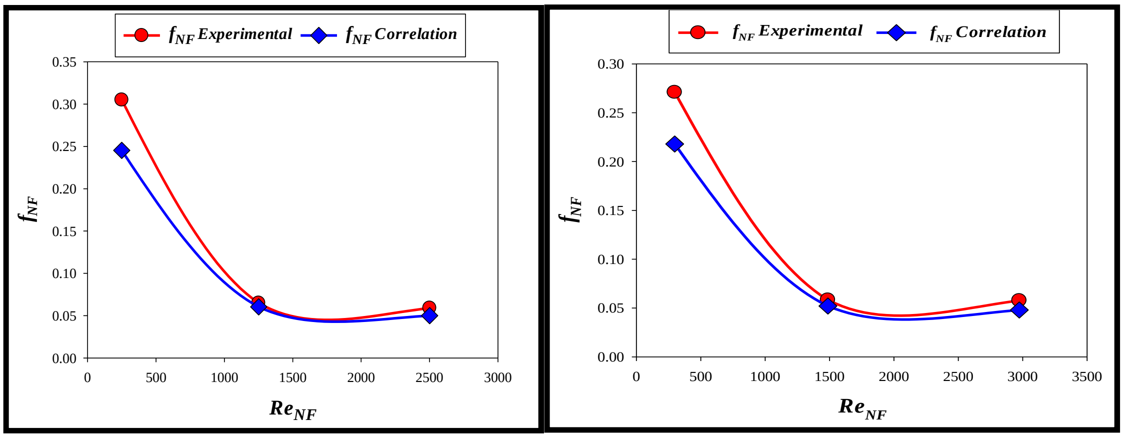

Figure 7. Comparison between the friction coefficient values versus the tubular Reynolds number of experimental and correlations results for the smooth tube: (a) experiments at $T_{t,i}$ = 40 °C, (b) experiments at $T_{t,i}$ = 50 °C.

3. RESULTS AND DISCUSSION

In this section, we present a bench of thermal parameters for four different types of double-tube heat exchangers: one using water, one using nanofluid, one using water with PF inserted in the annulus, and one using nanofluid with PF inserted in the annulus. The main results for each type of heat exchanger are the overall heat-transfer coefficient, heat transfer (Nusselt number), friction factor (f), and thermal performance factor (TPF) of the tube-side as a function of the tubular Reynolds number.

In this study, the following experimental designs were used:

- The air inlet temperature is maintained at 22.5 °C, and the flow rate is maintained at 1250 L/min.
- The nanofluid's inlet temperature are 40 and 50 °C, respectively.
- In both finned tube and plain circular tube heat exchangers, experiments are carried out at flow rates of 0.2, 1, and 2 L/min at a constant volumetric concentration of nanofluid.

3.1 Results of the Overall Heat Transfer Coefficient (U_i) (W/m^2.K°)

Figure 8 displays the experimental total heat transfer coefficient of water and nanofluid at different input temperatures as a function of Reynolds number at plain and fins tube heat exchangers.

Heat exchangers that employ fins and nanofluids have a greater total heat transfer coefficient compared to those that use water or nanofluids alone, as seen in the above figure, which increases as the Reynolds number climbs.

3.2 Results of Nusselt Number (Nu_t)

Figure 9 shows the experimental Nusselt number of the Fe_3O_4 -water nanofluid at various temperatures as a function of Reynolds number.

For nanofluid temperatures of 40 and 50°C, the Nusselt number determined from a smooth heat exchanger is significantly lower than that from a finned tube heat exchanger. It can be noticed from the figure that the Nusselt number of nanofluids increases with increasing Reynolds numbers.

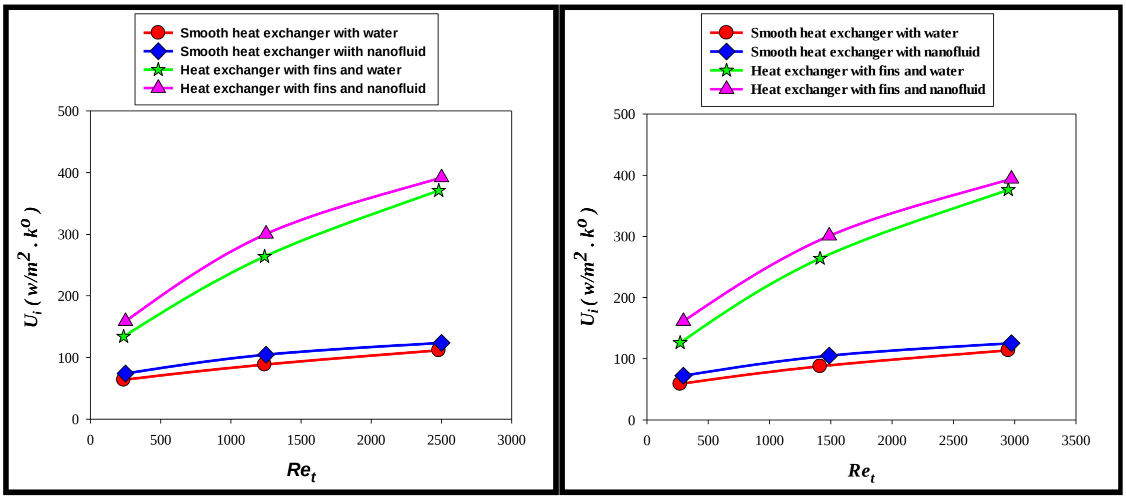

Figure 8. The overall heat transfer coefficient versus Re for the tube side for all cases. Experiments at (a) $T_{t,i}$ = 40°C, (b) $T_{t,i}$ = 50°C.

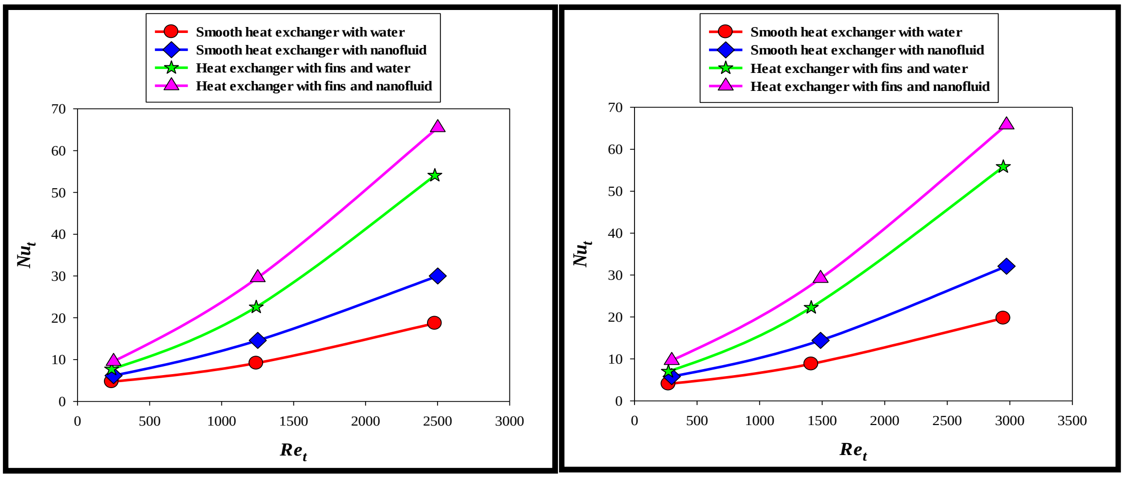

Figure 9. The Nusselt number vs Re for the tube side for experiments at (a) $T_{t,i}$ = 40°C, (b) $T_{t,i}$ = 50°C.

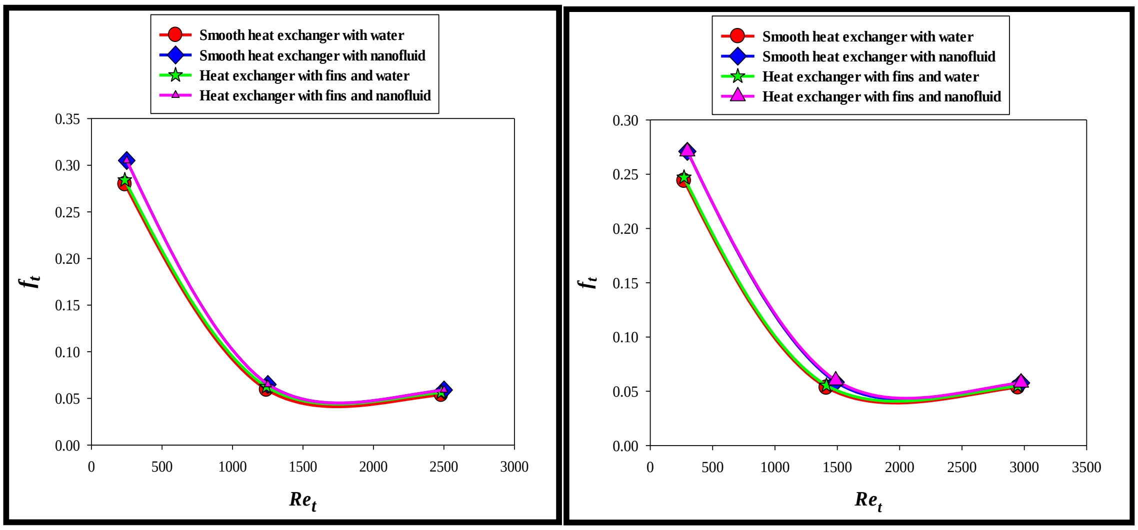

Figure 10. Friction factor vs Re for the tube side for all cases at (a) $T_{t,i}$ = 40°C, (b) $T_{t,i}$ = 50°C.

3.3 Results of Friction Factor (f_t)

Because it is closely linked to pumping power needs, which could determine whether utilizing a specific nanofluid is feasible, the friction factor is a crucial component.

Estimated friction factor in heat exchanger with fins and nanofluid is not much higher compared to smooth heat exchanger at different Reynolds numbers.

3.4 Evaluation of Thermal Performance Factors (*TPF*)

This heat transfer improvement's efficacy may be measured by the thermal performance factor (TPF). Assuming a fixed Reynolds number, passive approaches such as incorporating nanofluids or fins into the heat exchanger should result in a higher increase in convective heat transfer than the corresponding rise in fluid pressure drop. Under conditions of constant pumping power, the assessment was conducted using equation (19). one possible way to look at (TPF) is as the ratio of the increase in friction factor to the increase in heat transmission. This investigation began with a water-based smooth heat exchanger (TPF = 1) as its baseline state.

The figure should indicate the variation of TPF with Reynolds number (Re) of the tube-side of the heat exchanger for each of the following scenarios: double-tube heat exchanger by nanofluid, double-tube heat exchanger by water and (PF) inserted in the annulus, and double-tube heat exchanger by nanofluid and (PF) inserted in the annulus.

According to the results, given a constant volumetric concentration of nanofluid at varying Reynolds numbers, the finned tube heat exchanger has a 90–95% higher thermal performance factor than the plain tube heat exchanger.

coefficient and flow parameters. The following findings have been reached by us.

1. The nanofluid of Fe_3O_4 and water has far greater heat transfer coefficients than the base fluid alone.
2. The higher heat transfer rate of the finned tube heat exchanger is caused by the shape of the fins and the presence of nanofluids.
3. The heat transfer rate of the finned tube heat exchanger is 90-95% higher than that of the plain tube heat exchanger for a 0.5% Fe_3O_4-water nanofluid at different temperatures.
4. Heat exchangers containing nanofluids or fins have a greater overall heat transfer coefficient compared to those containing water or a smooth nanofluid, and this increase is proportional to the Reynolds number.
5. The Nusselt number computed from the smooth heat exchanger is much smaller than the one from the finned tube heat exchanger for nanofluid temperatures of 40 and 50°C.
6. For the same kind of fluid, finned or finless tubes have a higher friction factor than plain tubes; nevertheless, this factor drops with increasing nanofluid volumetric concentration and Reynolds number.

Finally, the results indicate that particle sedimentation, clogging, erosion, stability, and an increase in pressure drop are some disadvantages of employing higher particle sizes. increasing heat conductivity while maintaining the ideal volume concentration. Prior research has mostly concentrated on increasing the rate of heat transfer, with little regard for pressure drop. Thus, it is recommended that in addition to improving the heat transfer rate, the effect of combined passive approaches on pumping power be ascertained and thoroughly studied.

More thorough research on nanofluids and the

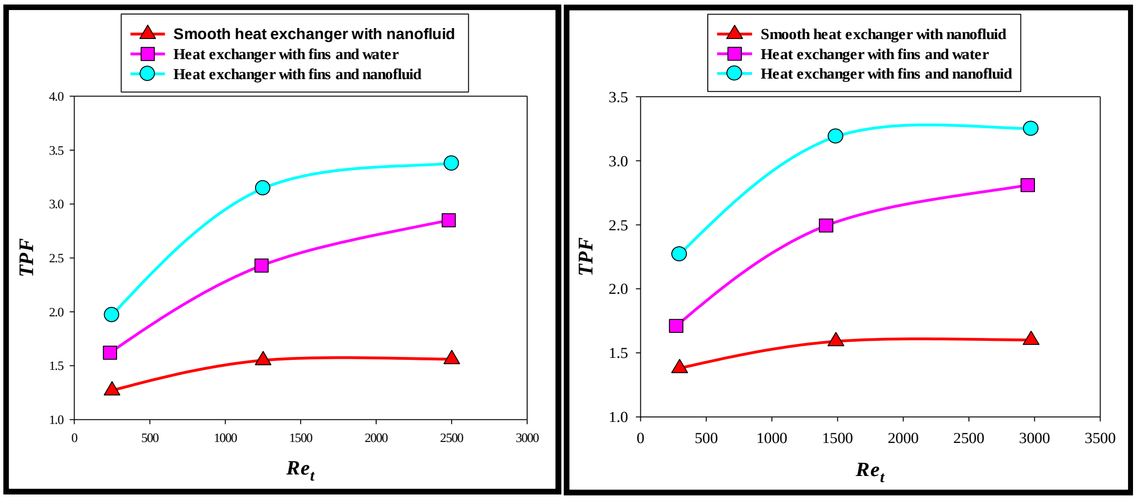

Figure 11. Thermal Performance Factor (*TPF*) and Re for the tube side for all cases: Experiments at (a) $T_{t,i}$ = 40°C, (b) $T_{t,i}$ =50°C.

4. CONCLUSIONS

For the tests, laminar flow conditions were utilized. We looked at the relationship between the flow Reynolds number, the nanofluid temperature, the air temperature, and the flow rate to determine the total heat transfer

functionality of liquid-air heat exchangers containing them is needed in the future. because the findings show that variables' measurement is significantly impacted by elements such as use of internal fins in tubes of heat exchangers, preparation methods, nanoparticle type, and surfactants. Consequently, these elements have a substantial impact on the outcomes and prevent the right results from being produced if they are disregarded. Therefore, it is advised to thoroughly consider and measure every component and to avoid making assumptions that are too simple.

NOMENCLATURE

A	Surface area of the cross-section duct (m^2)
C_p	Specific heat (kJ kg^{-1} K^{-1})
D_h	Hydraulic diameter (m)
h	Average convective heat transfer coefficient (W m^{-2} K^{-1})
k	Thermal conductivity (W m^{-1} K^{-1})
L	Channel length (m)
Nu	Nusselt number
Pr	Prandtl number
q"	Heat flux (W m^{-2})
Re	Reynolds number
T_b	Bulk temperature (K)
T_w	Wall temperature (K)
V	Average fluid velocity (m s^{-1})
x	Axial length (m)

Greek letters

μ	Viscosity (Pa s)
φ	Volumetric nanoparticle concentration (%)
ρ	Density (kg m^{-3})

Subscripts

nf	Nanofluid
bf	Base fluid
np	Nanoparticle
w	Wall
in	Inlet
out	Outlet
f	Fluid

DECLARATION OF ETHICAL STANDARDS

The author(s) of this article declare that the materials and methods used in this study do not require ethical committee permission and/or legal-special permission.

AUTHORS' CONTRIBUTIONS

Fauzi SHTEWİ: Conceptualization, performed the experiments and analysis the results.
Mehmet ÖZKAYMAK: Conceptualization, review of the manuscript, and supervision administration.
Khaled HAGİG: Theoretical studies, literature research.
Abdelkerim FAHED: Validation, Data Curation, Writing-original draft.
Faruk KİLİC: Contributed to performing experimental setup.
Mustafa GOKTAS: Reported the experimental results.
Nurettin ELTUGRAL: Contributed to preparing nanofluid.
Mustafa AKTAS: Conceptualization performed the experiments.

CONFLICT OF INTEREST

There is no conflict of interest in this study

REFERENCES

[1] A. P. Watkinson, M. Dl, and K. GR, "Heat transfer and pressure drop of internally finned tubes in turbulent air flow," 1975.

[2] A. P. Watkinson, D. L. Miletti, and P. Tarassoff, "Turbulent heat transfer and pressure drop in internally finned tubes," in ***AIChE Symposium Series***, 94–103,(1973).

[3] J. C. Maxwell, "A treatise on electricity and magnetism," ***Clarendon Press google Sch.,*** 2: 3408–3425,(1873).

[4] M. S. Baba, M. B. Rao, and A. Raju, "Experimental study of convective heat transfer in a finned tube counter flow heat exchanger with Fe3O4, water nanofluid," ***Int. J. Mech. Eng. Technol.,*** 500, (2017).

[5] M. S. Baba, A. V. S. R. Raju, and M. B. Rao, "Heat transfer enhancement and pressure drop of Fe3O4-water nanofluid in a double tube counter flow heat exchanger with internal longitudinal fins," ***Case Stud. Therm. Eng.,*** 12: 600–607, (2018).

[6] A. Zamzamian, S. N. Oskouie, A. Doosthoseini, A. Joneidi, and M. Pazouki, "Experimental investigation of forced convective heat transfer coefficient in nanofluids of Al2O3/EG and CuO/EG in a double pipe and plate heat exchangers under turbulent flow," ***Exp. Therm. Fluid Sci.***, 35(3): 495–502, (2011).

[7] I. Alam and P. S. Ghoshdastidar, "A study of heat transfer effectiveness of circular tubes with internal longitudinal fins having tapered lateral profiles," ***Int. J. Heat Mass Transf.,*** 45(6):1371–1376, (2002).

[8] M. R. Hajmohammadi, "Design and analysis of multi-scale annular fins attached to a pin fin," ***Int. J. Refrig.,*** 88: 16–23, (2018).

[9] R. L. Webb and M. J. Scott, "A parametric analysis of the performance of internally finned tubes for heat exchanger application," (1980).

[10] C.-C. Wang, W.-S. Lee, and W.-J. Sheu, "A comparative study of compact enhanced fin-and-tube heat exchangers," ***Int. J. Heat Mass Transf.,*** 44(18): 3565–3573, (2001).

[11] M. S. Kamel, R. A. Syeal, and A. A. Abdulhussein, "Heat transfer enhancement using nanofluids: a review of the recent literature," ***Am. J. Nano Res. Appl.***, 4(1):1–5, (2016).

[12] T. W. H. Sheu and S. F. Tsai, "A comparison study on fin surfaces in finned tube heat exchangers," *Int. J. Numer.* ***Methods Heat Fluid Flow,*** 9(1): 92–106, (1999).

[13] M. R. Hajmohammadi, "Optimal design of tree-shaped inverted fins," ***Int. J. Heat Mass Transf.***, 116:1352–1360, (2018).

[14] J. H. Masliyah and K. Nandakumar, "Heat transfer in internally finned tubes," (1976).

[15] M. R. Hajmohammadi, P. Alipour, and H. Parsa, "Microfluidic effects on the heat transfer enhancement and optimal design of microchannels heat sinks," ***Int. J. Heat Mass Transf.,*** 26:808–815, (2018).

[16] W. Duangthongsuk and S. Wongwises, "An experimental study on the heat transfer performance and pressure drop of TiO2-water nanofluids flowing under a turbulent flow regime," ***Int. J. Heat Mass Transf.***, 53(1-3):334–344, (2010).

[17] D. Wen and Y. Ding, "Experimental investigation into convective heat transfer of nanofluids at the entrance region under laminar flow conditions," ***Int. J. Heat Mass Transf.,*** vol. 47(24):5181–5188, (2004).

[18] L. S. Sundar, M. T. Naik, K. V Sharma, M. K. Singh, and T. C. S. Reddy, "Experimental investigation of forced

convection heat transfer and friction factor in a tube with Fe3O4 magnetic nanofluid," ***Exp. Therm. Fluid Sci***., 37: 65–71, (2012).

[19] W. Yu, H. Xie, L. Chen, and Y. Li, "Enhancement of thermal conductivity of kerosene-based Fe3O4 nanofluids prepared via phase-transfer method," ***Colloids surfaces A Physicochem. Eng. Asp.***,355(1–3): 109–113, (2010).

[20] L. S. Sundar, M. K. Singh, and A. C. M. Sousa, "Investigation of thermal conductivity and viscosity of Fe3O4 nanofluid for heat transfer applications," ***Int. Commun. heat mass Transf.,*** 44:7–14, (2013).

[21] F. W. Dittus and L. M. K. Boelter, "Heat transfer in automobile radiators of the tubular type," ***Int. Commun. heat mass Transf***., 12(1): 3–22, (1985).

[22] S. J. Kline, "Describing uncertainties in single-sample experiments," ***Mech. Eng.,*** 75:3–8, (1963).

[23] E. N. Sieder and G. E. Tate, "Heat transfer and pressure drop of liquids in tubes," ***Ind. Eng. Chem***., 28(12):1429–1435, (1936).

[24] V. Gnielinski, "New equations for heat and mass transfer in turbulent pipe and channel flow," ***Int. Chem. Eng.,*** vol. 16(2):359–367, (1976).

[25] G. F. Hewitt, G. L. Shires, and T. R. Bott, *Process Heat Transfer*. Behel House, (2000). [Online]. Available: **https://books.google.com.tr/book**s?id=OztADyim4XcC

[26] G. K. Filonenko, "Hydraulic resistance in pipes," (1954).